Original Article

Spironolactone Modulates Expressions of Cardiac Mineralocorticoid Receptor and 11β-Hydroxysteroid Dehydrogenase 2 and Prevents Ventricular Remodeling in Post-Infarct Rat Hearts

Mitsuo TAKEDA[1)], Tetsuya TATSUMI[1)], Shinsaku MATSUNAGA[1)], Hironori HAYASHI[1)], Masaki KIMATA[1)], Shoken HONSHO[1)], Susumu NISHIKAWA[1)], Akiko MANO[1)], Jun SHIRAISHI[1)], Hiroyuki YAMADA[1)], Tomosaburo TAKAHASHI[1)], Satoaki MATOBA[1)], Miyuki KOBARA[2)], and Hiroaki MATSUBARA[1)]

Aldosterone antagonists have been reported to prevent ventricular remodeling after myocardial infarction (MI) *via* their action to extracellular matrix (ECM). However, it remains largely unknown whether aldosterone antagonists attenuate myocyte loss in the remodeling process. The present study examined whether spironolactone prevents myocyte apoptosis and improves post-infarct ventricular remodeling in rats. MI was achieved by permanent occlusion of the left coronary artery. Administration of spironolactone (100 mg/kg/day) was started immediately after MI. Sprague-Dawley rats were divided into four groups: 1) sham, 2) spironolactone-treated sham, 3) untreated MI, 4) spironolactone-treated MI. Echocardiographic parameters (left ventricular [LV] diastolic dimension [LVDd], fractional shortening [%FS]), hemodynamic parameters (LV systolic pressure [LVSP], LV end-diastolic pressure [LVEDP], dP/dt_{max} and dP/dt_{min}) and collagen accumulation quantitated by Masson's Trichrome staining were significantly improved in the spironolactone-treated MI group on the 14th day, compared with the untreated MI group. Moreover, the percentage of apoptotic myocytes evaluated by terminal deoxynucleotide transferase–mediated dUTP nick end labeling (TUNEL) assay was significantly lower in the spironolactone-treated MI group on the 2nd (3.54% *vs.* 5.79% in untreated MI group), 7th (0.65% *vs.* 1.37% in untreated MI group) and 14th days (0.11% *vs.* 0.16% in untreated MI group). Real time reverse transcription–polymerase chain reaction (RT-PCR) analysis showed that the expression of mineralocorticoid receptor (MR) mRNA and that of 11β-hydroxysteroid dehydrogenase 2 (11β-HSD2) mRNA, which is known to confer aldosterone selectivity on MR, were upregulated in the untreated MI group, and that spironolactone significantly suppressed the expression of these genes. Moreover, spironolactone significantly inhibited aldosterone-induced apoptosis in cultured rat cardiac myocytes in a dose-dependent fashion. Our study demonstrates that, in addition to their effect on ECM, aldosterone antagonists inhibit myocyte apoptosis and prevent post-infarct ventricular remodeling by modulating the expression levels of MR and 11β-HSD2, which are enhanced in the remodeling heart. (*Hypertens Res* 2007; 30: 427–437)

***Key Words*: aldosterone, apoptosis, heart failure, myocardial infarction, remodeling**

From the [1)]Department of Cardiovascular Medicine, Kyoto Prefectural University School of Medicine, Kyoto, Japan; and [2)]Department of Clinical Pharmacology, Kyoto Pharmaceutical University, Kyoto, Japan.

This study was supported in part by Grants-in-Aid for Scientific Research from the Ministry of Education, Science and Culture and from the Ministry of Health, Labor and Welfare of Japan.

Address for Reprints: Tetsuya Tatsumi, M.D., Ph.D., Department of Cardiovascular Medicine, Kyoto Prefectural University School of Medicine, Kawaramachi-Hirokoji, Kamigyo-ku, Kyoto 602–8566, Japan. E-mail: tatsumi@koto.kpu-m.ac.jp

Received April 21, 2006; Accepted in revised form December 20, 2006.

Introduction

Extensive myocardial infarction (MI) often causes severe congestive heart failure with left ventricular (LV) remodeling, which is characterized by a ventricular dilatation and diminished cardiac performance (*1*). Cardiac myocytes are known to undergo apoptosis under some pathological conditions, such as hypoxia and ischemia-reperfusion (*2*, *3*). Indeed, recent reports suggest that apoptosis contributes significantly to progressive loss of cardiac myocytes during and after MI (*4–6*) and, more importantly, that apoptosis plays a crucial role in the development and progression of heart failure after MI (*7–9*).

A great body of evidence suggests that the renin-angiotensin-aldosterone system (RAAS) plays important roles in the regulation of cardiovascular homeostasis and in the pathogenesis of a variety of cardiovascular diseases (*10*, *11*). Although aldosterone classically promotes unidirectional transepithelial sodium transport, thereby regulating blood volume and blood pressure (BP), recent clinical and experimental studies have indicated that aldosterone receptor antagonists, such as spironolactone and eplerenone, dramatically reduce morbidity and mortality from heart failure (*12*, *13*). Moreover, myocardial production of aldosterone has been found in previous clinical and experimental studies (*14–16*). Aldosterone interacts with mineralocorticoid receptors (MR) to promote endothelial dysfunction, facilitate thrombosis, reduce vascular compliance, impair baroreceptor function and cause myocardial and vascular hypertrophy as well as fibrosis with the promotion of pathological remodeling (*17*). Mineralocorticoid receptor and 11β-hydroxysteroid dehydrogenase 2 (11β-HSD2), which confers mineralocorticoid selectivity to aldosterone target tissues, have also been detected in hearts, suggesting that aldosterone has direct roles in the cardiovascular system (*18*, *19*).

Recently, we have demonstrated that aldosterone accelerates the mitochondrial apoptotic pathway through calcineurin activation and BAD dephosphorylation, and we have suggested that the proapoptotic action of aldosterone may directly contribute to the progression of heart failure (*20*). However, little is known about the roles of aldosterone and MR signaling in mediating adverse remodeling in response to MI. The present study was therefore designed to determine whether the tissue aldosterone system is also activated in MI and whether spironolactone, an aldosterone antagonist, prevents myocyte apoptosis and improves post-infarct ventricular remodeling in rats. We found that the expression of MR mRNA and that of 11β-HSD2 mRNA were significantly upregulated in MI, and that spironolactone can inhibit myocyte apoptosis and prevent post-infarct ventricular remodeling by modulating the MR-mediated aldosterone signaling.

Methods

All animals were handled in accordance with the Guide for the Care and Use of Laboratory Animals published by the US National Institutes of Health (NIH publication No. 85-23, revised 1996). The protocol was approved by the Bioethics Committee of the Kyoto Prefectural University of Medicine.

Surgical Procedure and Study Protocols

MI were produced as described previously (*21*). Briefly, male Sprague-Dawley rats weighing 220 to 240 g were anesthetized with intraperitoneal sodium pentobarbital (30 mg/kg body weight). After thoracotomy at the fourth intercostal space, the heart was exteriorized, and the left proximal coronary artery was surgically occluded with a 6-0 silk ligature. The heart was then returned to its normal position, and the thorax was closed. Mortality was 30% within the first 24 h. Sham-operated control rats underwent the same surgical procedure but without occlusion of the coronary artery. Surviving MI rats were randomly allocated to one of four groups ($n=6$ per group): 1) sham (control), 2) spironolactone-treated sham, 3) untreated MI, 4) spironolactone-treated MI. Spironolactone (Nacalai Tesque, Tokyo, Japan) was dissolved in dimethyl sulfoxide (DMSO) and orally administered to the rats. Spironolactone treatment was started immediately after the surgical procedure and continued every day for 2 weeks. In sham and MI rats without spironolactone treatment, saline dissolved in DMSO was also orally administered as a vehicle. The dose of spironolactone (100 mg/kg per day) was determined from previous studies (*22*).

Hemodynamics and LV Function

Systolic BP was measured before and at 2, 7 and 14 days after surgery by tail-cuff plethysmography in conscious, lightly restrained animals.

A 2F micromanometer-tipped catheter (SPC-320, Millar Instruments, Houston, USA) was advanced from the right carotid artery into the left ventricle, and LV systolic pressure (LVSP), LV end-diastolic pressure (LVEDP) and maximal rates of pressure rise and decline (dP/dt_{max} and dP/dt_{min}, respectively) were measured at 14 days after MI under pentobarbital anesthesia (30 mg/kg body weight, intraperitoneally). All tracings were recorded on a physiological recorder, and the heart rate was obtained from an arterial pressure tracing.

All the experimental animals underwent echocardiography under pentobarbital anesthesia before and at 2, 7 and 14 days after surgery. The echocardiographic measurements were performed with the use of a 12 MHz ultraband sector probe (SONOS 5000, Hewlett-Packard, Palo Alto, USA). LV diastolic dimension (LVDd) and fractional shortening (%FS) were measured in the short-axis M-mode left parasternal projection at the mid-portion of the left ventricle.

Table 1. Time Course Changes of Body Weight, Heart Rate and Systolic Blood Pressure in Each Group

	Sham	Sham+Sp	MI	MI+Sp
Body weight (g)				
Before	225±2.7	222±1.1	226±2.0	223±1.7
Day 14	265±3.2	255±4.5	263±2.5	262±2.5
Heart rate (/min)				
Before	433±5.4	430±5.1	426±7.0	434±9.0
Day 14	423±11.2	410±25.1	415±11.3	430±20.2
Systolic BP (mmHg)				
Before	123±3.6	123±1.8	124±3.7	123±4.5
Day 2	125±3.1	122±2.6	103±2.1*	100±4.4*
Day 7	125±2.3	122±3.9	107±3.0*	106±3.9*
Day 14	126±2.1	121±3.5	108±2.7*	108±3.7*

BP, blood pressure; Sham, sham-operated rats; Sham+Sp, spironolactone-treated sham; MI, untreated rats with myocardial infarction; MI+Sp, spironolactone-treated rats with myocardial infarction. Each value represents a mean±SEM. These parameters were measured as described in Methods. *$p<0.05$ *vs*. either Sham or Sham+Sp.

Planimetry of Infarct Size, LV Remodeling and Myocardial Fibrosis

The left ventricle was cut transversely at mid level. Formalin-fixed, paraffin-embedded tissue samples were cut into 4 μm sections and stained with Masson's Trichrome. Infarct size was determined planimetrically as the ratio of infarct tissue or scar tissue to the length of the entire LV endocardial circumference (*23*). To quantitate wall thinning, the free-wall thickness was measured at the thinnest point of transmural infarction from the section at the mid-LV level. The septal wall from the same slide at the point on the septum diametrically opposed to the point used for infarct thinning. The infarct wall-thinning ratio was then calculated as free wall/septal wall, as previously described (*24*).

The percentage of area occupied by collagen as opposed to noncollagenous tissue was quantitated in sections stained with Masson's Trichrome using NIH Image densitometry at 14 days after the MI procedure (*25*). Collagen volume fraction was calculated as the sum of all collagen-positive areas divided by the sum of muscle areas and collagen areas.

Myocardial Apoptosis

Each deparaffinized tissue section was treated with 0.3% H_2O_2 in 100% methanol to inhibit endogenous peroxidase activity and then incubated with normal goat serum for 20 min at room temperature. The terminal deoxynucleotide transferase–mediated dUTP nick end labeling (TUNEL) assay was performed to detect apoptotic cells (ApopTag kit, Chemicon International, Temecula, USA), as previously described (*21*). Myocytes were immunohistochemically stained with anti–myosin heavy chain antibody (CLA67/1; BD Transduction Laboratories, San Jose, USA) using Histofine Simple Stain MAX PO® as a secondary antibody (Nichirei, Tokyo, Japan). In brief, specimens were incubated with a primary antibody for 60 min. Then they were incubated with Universal Immuno-peroxidase Polymer (Nichirei) conjugated with anti-rabbit antibodies and peroxidases for 10 min. Color was developed using aminoethylcarbazole (AEC) for 10 min. Finally, specimens were counterstained with hematoxylin to visualize the nuclei. Specimens were washed three times with PBS containing 0.1% Tween-20 between steps. Apoptotic myocytes were then identified as TUNEL-positive and reddish-brown stained cells. The percentage of apoptotic myocytes was the proportion of TUNEL-positive myocytes from the total number of myocytes. Because TUNEL-positive myocytes were detected only in the border zone of the infarct area, analyses were performed from 2,000 myocytes counted in this area.

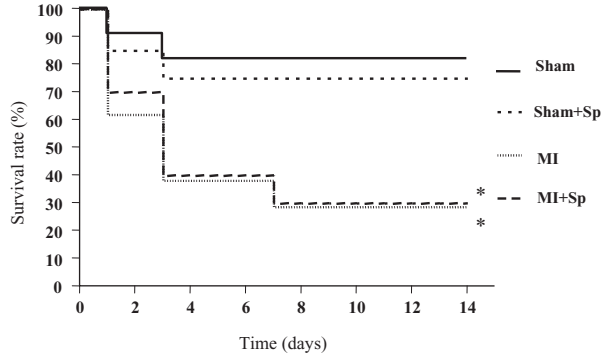

Fig. 1. *Survival curves of post-infarct rats. Spironolactone treatment was started immediately after MI and continued for 2 weeks. *$p<0.05$ vs. either Sham or Sham+Sp.*

Quantification of Cardiac Gene Expression

Total RNA was extracted from the hearts, and cDNA was synthesized from 1 μg of total RNA with the SuperScript III

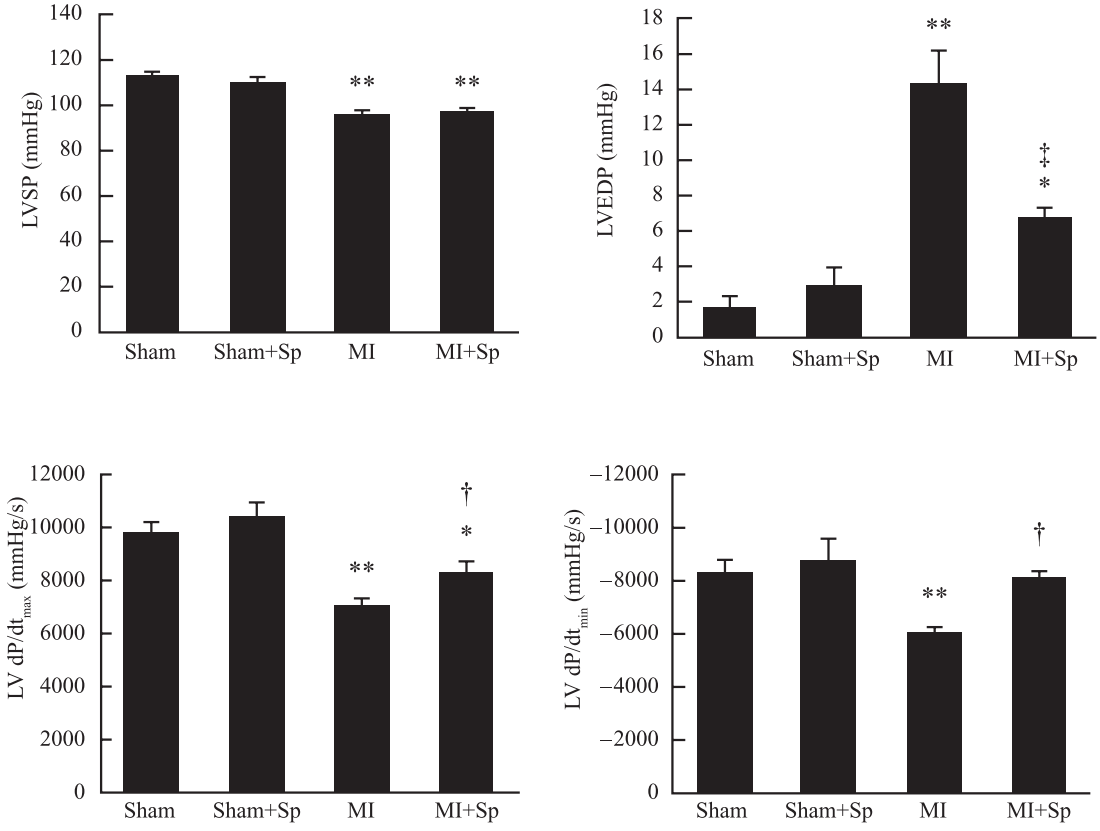

Fig. 2. *Hemodynamic measurements obtained at 14 days after surgery. LVSP, left ventricular systolic pressure; LVEDP, left ventricular end-diastolic pressure; dP/dt_{max}, maximal rate of pressure rise; dP/dt_{min}, maximal rate of pressure decline; Sham, sham-operated rats; Sham+Sp, spironolactone-treated Sham; MI, untreated rats with myocardial infarction; MI+Sp, spironolactone-treated rats with myocardial infarction. The parameters were measured as described in Methods. *$p < 0.05$ vs. either Sham or Sham+Sp, **$p < 0.01$ vs. either Sham or Sham+Sp, $^{\dagger}p < 0.05$ vs. MI, $^{\ddagger}p < 0.001$ vs. MI.*

First-Strand Synthesis System for reverse transcription (RT)–polymerase chain reaction (PCR) (Invitrogen, Carlsbad, USA). Target cDNA levels were analyzed by quantitative real-time kinetic PCR using TaqMan PCR master mix and TaqMan Gene Expression Assays (Applied Biosystems, Foster City, USA) with the ABI Prism 7700 Sequence Detector system (Applied Biosystems). 18S rRNA was used for normalization between samples, and the comparative threshold (C_T) method was used to assess the relative abundance of the targets (*26*). The TaqMan Gene Expression Assays used were: 11β-HSD2 (Rn00492539_m1), mineral corticoid receptor (Nr3c2) (Rn00565562_m1), collagen I (Col1aI) (Rn01463848_m1) and 18S rRNA (4319413E).

Cultured Neonatal Rat Cardiac Myocytes

Primary cultures of neonatal rat cardiac myocytes were prepared from neonatal Wistar rat hearts by digestion with 0.2% collagenase as described previously (*20*). The myocyte-rich fraction (separated by Percoll gradient) was resuspended in Dulbecco's modified Eagle's medium (DMEM) supplemented with 10% fetal bovine serum (FBS). Myocytes were cultured by bromodeoxyuridine (BrdU; 10^{-4} mol/L) during the first 48 h and were then incubated in DMEM containing 0.5% FBS without BrdU. All experiments were performed 36 to 48 h after this incubation.

In Vitro Effect of Spironolactone on Myocyte Apoptosis

According to our previous report, myocyte apoptosis was induced by 10^{-5} mol/L aldosterone for 24 h (*20*). To investigate the dose-dependent effects of spironolactone on aldosterone-induced apoptosis, myocytes were incubated with spironolactone (10^{-8}–10^{-5} mol/L) in the presence of 10^{-5} mol/L aldosterone for 24 h. Control myocytes were incubated in serum-free DMEM but were not treated with aldosterone. Myocytes were histochemically stained as previously described (*20*). The cells were visualized by fluorescein microscopy, and the images were generated by dual-exposure photography. Apoptotic cells were identified on the basis of distinctive condensed or fragmented nuclear morphology,

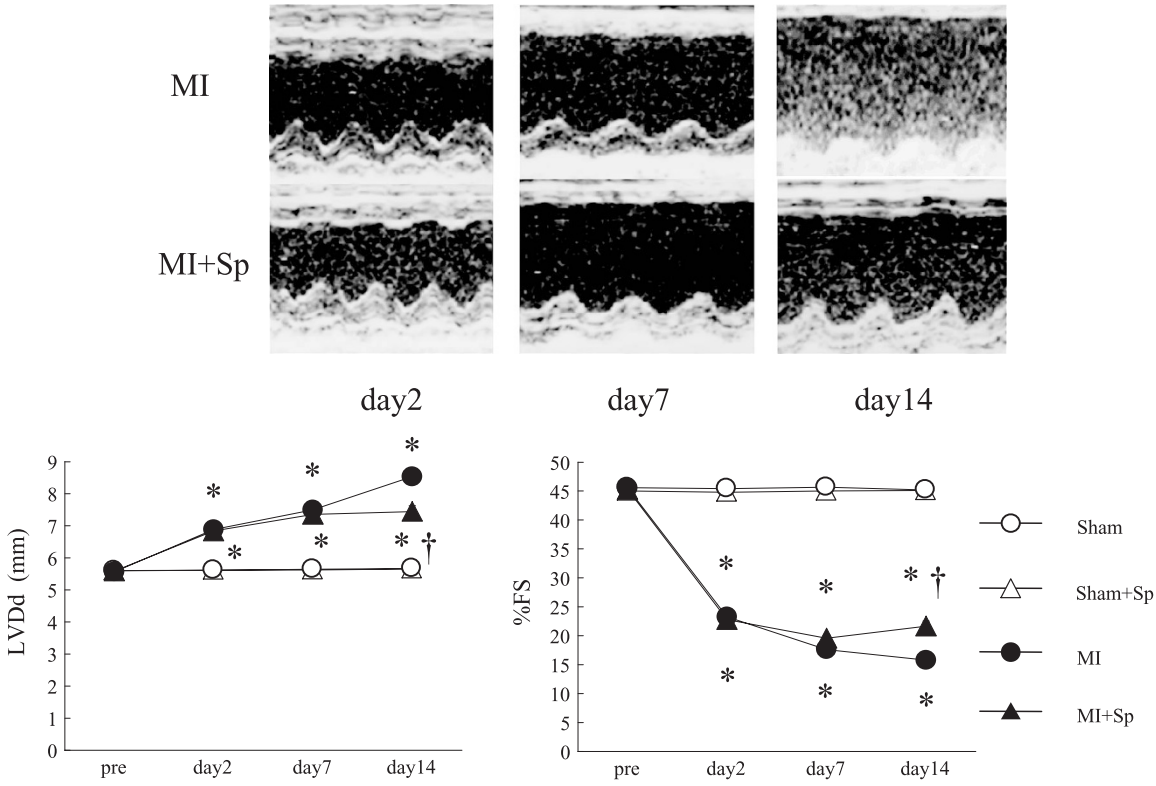

Fig. 3. *Effects of spironolactone on LV function assessed by echocardiography. LVDd, left ventricular diastolic dimension; %FS, fractional shortening. These parameters were determined as described in Methods. Upper panels show representative recordings obtained from untreated MI and spironolactone-treated MI rats. Lower panels show time course changes of LVDd and %FS in each group. *$p < 0.001$ vs. either Sham or Sham+Sp, †$p < 0.001$ vs. MI.*

and apoptotic cell counts were expressed as percentages of the total numbers of nuclei counted.

Statistical Analysis

All values are expressed as means±SEM. Differences in systolic BP and echocardiographic measurements were compared by repeated measures analysis of variance (ANOVA) with a post hoc test using Bonferroni's multiple comparison tests. For comparisons of hemodynamic measurements, infarct size, LV wall-thinning ratio, myocardial fibrosis, and the percentage of myocyte apoptosis among groups, one-way ANOVA and Bonferroni's multiple comparison tests were performed. A p-value of <0.05 was considered to indicate statistical significance.

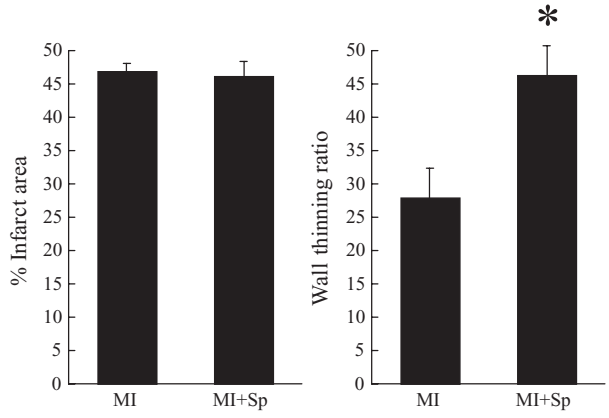

Fig. 4. *Effects of spironolactone on % infarct area and wall-thinning ratio in untreated MI and spironolactone-treated MI rats at 14 days after surgery. The parameters were determined as described in Methods. *$p < 0.01$ vs. MI.*

Results

Hemodynamics and Survival Rate

Time course changes in body weight, heart rate, and systolic BP are shown in Table 1. Body weight and heart rate did not significantly change among the four groups. Spironolactone (100 mg/kg per day) did not significantly lower the systolic BP of sham-operated control rats throughout the experimental period. Although systolic BP was significantly reduced to

≈0.8-fold that of the control at 2 days after coronary artery occlusion and remained low thereafter in MI rats, there were no significant differences in BP between the untreated MI and spironolactone-treated MI groups.

Figure 1 shows the survival rates among the four groups. MI significantly decreased the survival rate, compared with sham or spironolactone-treated sham rats. Administration of spironolactone, begun immediately after MI and continued for 2 weeks, did not significantly affect the surviving rates; the 2-week survival rate of the spironolactone-treated MI rats was 30%, compared with 28.6% for the untreated MI rats. Figure 2 illustrates the LVSP, LVEDP, dP/dt_{max} and dP/dt_{min} in the four groups at 14 days after surgery. Although MI reduced LVSP to ≈0.9-fold that of the control, spironolactone treatment did not significantly affect LVSP. The untreated MI rats had a markedly elevated LVEDP (14.3±1.9 mmHg) compared with the control (1.0±0.7 mmHg). Spironolactone treatment did not affect LVEDP in control rats (2.8±1.0 mmHg); however, it significantly attenuated the MI-induced rise in LVEDP (6.7±0.6 mmHg, $p<0.001$ *vs*. untreated MI). The dP/dt_{max} and dP/dt_{min} in untreated MI rats were significantly decreased, to 0.71-fold and 0.72-fold those of the control, respectively. Although spironolactone alone did not affect dP/dt_{max} or dP/dt_{min} in control rats, it significantly enhanced both, to 0.85-fold ($p<0.05$ *vs*. untreated MI) and 0.98-fold ($p<0.01$ *vs*. untreated MI) those of the control, respectively.

LV Remodeling and Function

To characterize the changes in LV function and geometry after MI, echocardiographic parameters (LVDd, %FS) were measured before and at 2, 7 and 14 days after surgery (Fig. 3). After MI, LVDd increased gradually, from 5.6±0.1 mm to 8.5±0.1 mm, and %FS decreased progressively, from 45.5±0.8% to 15.8±1.0%, whereas spironolactone treatment inhibited the MI-induced incline in LVDd (from 5.6±0.1 mm to 7.4±0.2 mm) and improved the MI-induced decline in %FS (from 45.3±0.8% to 21.6±0.9%). At 14 days after surgery, LVDd was significantly smaller and %FS was significantly greater in the spironolactone-treated MI group than in the untreated MI group.

Infarct area assessed by planimetry was similar between the untreated MI group (46.9±1.1%) and the spironolactone-treated MI group (46.1±2.2%) at 14 days after surgery (Fig. 4). In contrast, the infarct wall-thinning ratio, an index of infarct expansion, was significantly greater in the spironolactone-treated MI group (46.3±4.4%, $p<0.05$) than in the untreated MI group (27.9±4.4%) at 14 days after surgery, while the wall-thinning ratio was not significantly different between these groups within 7 days after MI (data not shown).

Myocardial Fibrosis

Figure 5 illustrates the representative non-infarct myocardial sections stained with Masson's Trichrome and the percentages of interstitial fibrosis in the four groups. On histological examination at 14 days after surgery, the untreated MI rats showed significantly extensive interstitial fibrosis (6.1±0.5%) compared with the control (1.9±0.1%). Although spironolactone alone did not affect the collagen volume fraction in control rats, it decreased reactive interstitial fibrosis significantly, to 3.8±0.3% ($p<0.001$), compared with untreated MI rats.

Myocardial Apoptosis

Figure 6 shows the representative TUNEL staining and the percentage of apoptotic myocytes in untreated MI and spironolactone-treated MI groups. Apoptotic cells were rarely found in the control rats or in the non-infarct areas of the MI rats (data not shown). In contrast, the TUNEL-positive nuclei were observed mainly in the ischemic border zone and detected in both myocytes and non-myocytes. To distinguish the myocyte nuclei from the non-myocyte nuclei, we performed double immunohistochemical staining of cardiac myosin heavy chain (reddish brown) and apoptotic nuclei using TUNEL (brown) (Fig. 6, left). The percentage of apoptotic cardiac myocytes in the ischemic border zone increased to 5.79±0.37% at 2 days after MI and decreased thereafter to 1.37±0.10% and 0.16±0.01% at 7 and 14 days after MI, respectively. Spironolactone significantly inhibited the apoptotic cardiomyocytes to 3.54±0.26% ($p<0.001$), 0.65±0.06% ($p<0.001$) and 0.11±0.01% ($p<0.05$) at 2, 7 and 14 days after MI, respectively (Fig. 6, right).

Myocardial Gene Expression

The mRNA expression levels of collagen type I, MR and 11β-HSD2 analyzed by real-time RT-PCR are shown in Fig. 7. In untreated MI rats, collagen type I gene expression was significantly increased to 3.9-fold that of the control, whereas spironolactone significantly attenuated the rise in collagen type I gene expression to 2.14-fold that of the control. MR and 11β-HSD2 mRNA expression levels were also upregulated to 2.24-fold and 2.22-fold those of the control, respectively, in untreated MI rats. In contrast, spironolactone significantly suppressed the MR and 11β-HSD2 expression levels to 0.73-fold and 1.3-fold those of the control, respectively, although it did not affect the expression of these two genes in control rats.

In Vitro Effect of Spironolactone on Myocyte Apoptosis

Treatment of myocytes with 10^{-5} mol/L aldosterone increased the percentage of myocyte apoptosis significantly,

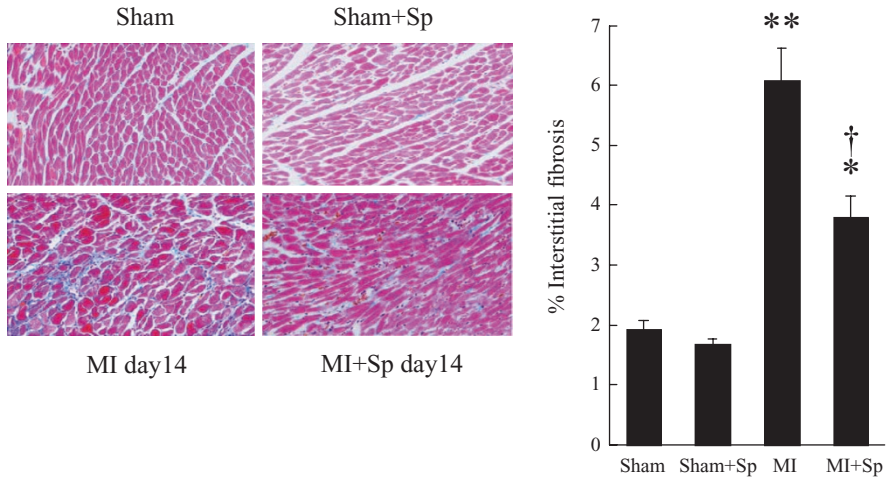

Fig. 5. *Histological analysis of 14-days post-infarct rat hearts. Histological specimens from non-infarct area were stained with Masson's Trichrome in each group. Left panel shows representative micrographs (magnification: ×100) and right panel shows % interstitial fibrosis calculated as the sum of all collagen-positive areas divided by the sum of muscle areas and collagen areas, as described in Methods. *p < 0.01 vs. either Sham or Sham+Sp, **p < 0.0001 vs. either Sham or Sham+Sp, †p < 0.001 vs. MI.*

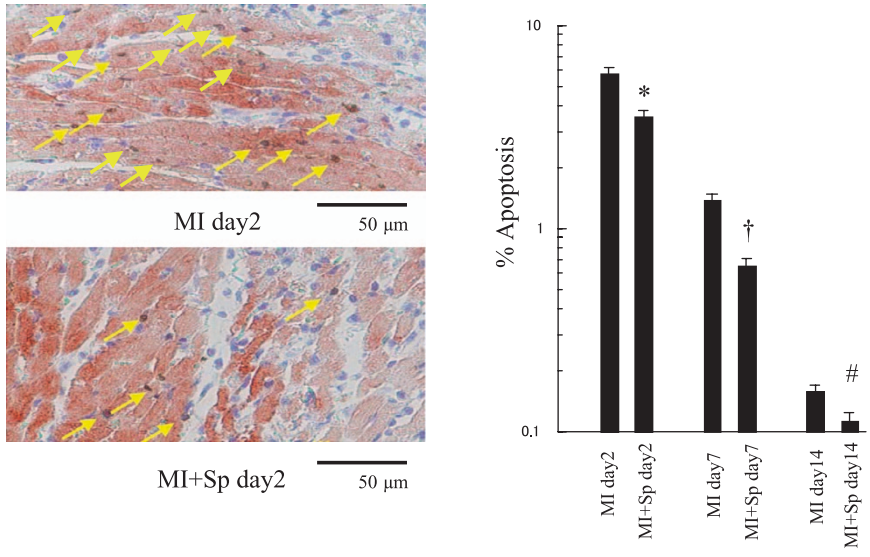

Fig. 6. *Histochemical characterization of apoptotic myocytes. Histological specimens from ischemic border zone in untreated MI and spironolactone-treated MI rats were stained with double immunohistochemical staining of cardiac myosin heavy chain (reddish brown) and apoptotic nuclei using TUNEL (brown), as described in Methods. Left panel shows representative micrographs (magnification: ×400) at 2 days after MI, and right panel shows time course changes in the percentage of apoptotic myocytes, calculated as described in Methods. *p < 0.001 vs. MI day 2, †p < 0.001 vs. MI day 7, #p < 0.05 vs. MI day 14.*

to 15.1±2.0%, as compared with serum-deprived control (7.9±1.3%) (Fig. 8). Spironolactone (10^{-8}–10^{-5} mol/L) inhibited myocyte apoptosis in a dose-dependent fashion, such that 10^{-6} and 10^{-5} mol/L spironolactone significantly reduced the percentage of apoptotic cells to 8.8±1.2% and 7.9±1.3%, respectively.

Discussion

The present study has shown that treatment of spironolactone started immediately after MI significantly improved myocardial function as assessed by hemodynamic and echocardiographic analyses, decreased collagen accumulation, and finally attenuated the LV remodeling process in post-infarct

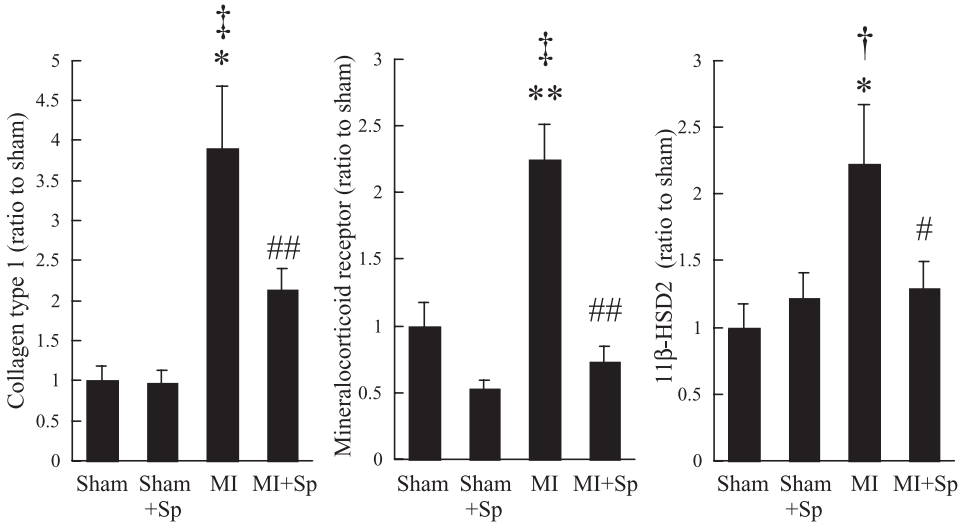

Fig. 7. *Messenger RNA expression levels of collagen type 1, mineralocorticoid receptor (MR) and 11β-hydroxysteroid dehydrogenase 2 (11β-HSD2). Total RNA was extracted from the hearts at 14 days after surgery, and cDNA were synthesized from 1 μg of total RNA by RT-PCR. Target cDNA levels were then analyzed by quantitative real-time kinetic PCR, as described in Methods. Each mRNA level is presented as a relative value with sham-operated rats. *$p < 0.01$ vs. Sham, **$p < 0.0001$ vs. Sham, †$p < 0.05$ vs. Sham+Sp, ‡$p < 0.0001$ vs. Sham+Sp, #$p < 0.05$ vs. MI, ##$p < 0.01$ vs. MI.*

rat hearts. Moreover, we have demonstrated for the first time that spironolactone significantly and continuously decreases the percentage of myocyte apoptosis in the infarct border zone from the early period after MI, as evaluated by TUNEL assay. Expression levels of MR and 11β-HSD2 mRNA were significantly increased after MI, and spironolactone treatment significantly inhibited the rise in these levels. Our data therefore suggest that, besides the action to the collagen volume fraction, aldosterone antagonist inhibits myocyte apoptosis and prevents post-infarct ventricular remodeling by modulating the expression levels of MR and 11β-HSD2, which are enhanced in the remodeling heart.

A growing body of evidence suggests that aldosterone mediates a variety of actions to the cardiovascular system and plays an important role in the process of ventricular remodeling independent of blood volume and BP (*27*, *28*). The present study showed that spironolactone significantly prevented the progression of LV systolic dysfunction, as evidenced by improvements in dP/dt_{max} and %FS, as well as the progression of LV diastolic dysfunction, as evidenced by improvement in dP/dt_{min}. Spironolactone also significantly attenuated the progressive enlargement of LV dimension (LVDd), infarct expansion (infarct wall-thinning ratio), and reactive interstitial fibrosis after MI. In a sense, our results suggest that aldosterone inhibition contributes to the attenuation of ventricular remodeling through the modification of extracellular matrix (ECM), consistent with the previous observations (*24*, *29–31*).

The accumulated data strongly suggest that apoptosis plays a pivotal role in the development and progression of heart failure after MI (*7–9*). Recently, Hayakawa *et al*. have demonstrated that intervention of apoptosis by a pancaspase inhibitor, Bos-Asp-fmk, improves LV remodeling and dysfunction by inhibiting granulation tissue cell apoptosis after MI (*32*). Wencker *et al*. (*33*) and Foo *et al*. (*34*) have reported that even the very low rate of 0.023% myocyte apoptosis is sufficient to cause lethal dilated cardiomyopathy in transgenic mice expressing inducible caspase-8. Cesselli *et al*. have also reported that myocyte apoptosis below 0.43% precedes ventricular dysfunction and correlates with the time-dependent deterioration of myocardial function in pacing-induced dog dilated cardiomyopathy (*35*). Chandrashekhar *et al*. have also reported that the reduction of apoptotic cells by caspase-1 inhibition improves systolic function and attenuates ventricular remodeling in rat infarct hearts (*36*).

The execution of infarct-related apoptosis is complexly regulated by several pathophysiological factors, including severity of ischemia, cellular energy levels, mechanical stress, and neurohormonal activation (*e.g.*, RAAS) (*2*, *3*, *37*). One factor that is particularly likely to drive infarct-associated apoptosis is aldosterone, because we have recently demonstrated that aldosterone can directly accelerate the mitochondrial apoptotic pathway in cultured rat cardiac myocytes (*20*). Moreover, in the present study we have demonstrated that spironolactone (10^{-7}–10^{-5} mol/L) significantly inhibited aldosterone-induced apoptosis in cultured cardiac myocytes in a dose-dependent fashion (Fig. 8). The present study, therefore, actually extends our previous *in vitro* hypothesis and strongly supports the notion that aldosterone antagonism inhibits myocyte apoptosis underlying the progression of post-infarct remodeling. Our data indicate that a ≈50–60% reduction of myocyte apoptosis by spironolactone

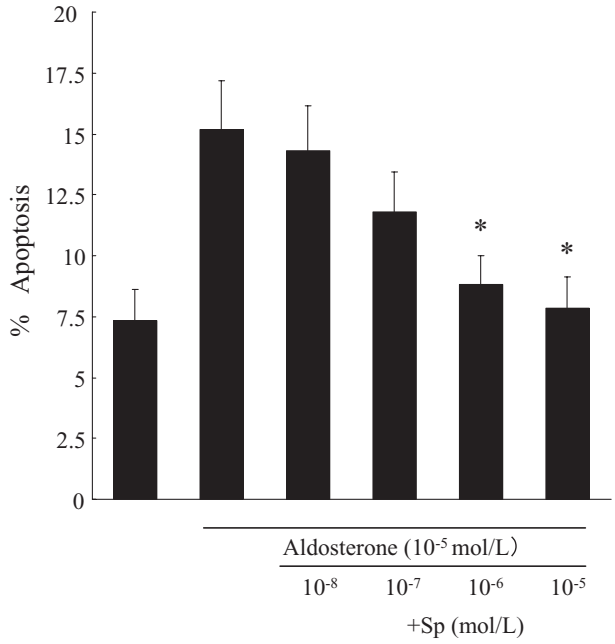

Fig. 8. *Effects of spironolactone on myocyte apoptosis induced by aldosterone. Cultured cardiac myocytes were incubated with spironolactone (10^{-8}–10^{-5} mol/L) in the presence of 10^{-5} mol/L aldosterone for 24 h, and the percentage of apoptotic myocytes was calculated as described in Methods. *$p < 0.01$ vs. Aldosterone (10^{-5} mol/L).*

treatment (Fig. 6) was associated with a 53% decrease in LVEDP (Fig. 2), a 41% increase in %FS, and a 13% decrease in LVDd (Fig. 3), compared with untreated MI rats. As the theoretical formula for the relationship between the suppression of LV remodeling and the anti-apoptotic effect has not been fully elucidated, this issue is a limitation of the present study. However, since the previous reports and our data show that infarct-associated myocyte apoptosis is associated with the remodeling process, it now appears very likely that the anti-apoptotic effect of aldosterone antagonist plays a pivotal role in the prevention of post-infarct ventricular remodeling. Moreover, in addition to its affinity for MR, prolonged administration of spironolactone is known to possess an affinity for androgen and progesterone receptors and to exert endocrine effects. However, since our experimental period of 2 weeks is relatively short, it is reasonable to consider that the present results are mainly derived from the aldosterone antagonistic action of spironolactone (*38*).

Accumulating evidence indicates that aldosterone is produced in cardiac tissues, particularly under pathological conditions. In view of the tissue-specific activation of myocardial aldosterone, Silvestre *et al*. have already reported that MI raises aldosterone synthase (CYP11B2) mRNA by 2.0-fold and the aldosterone level by 3.7-fold in rats (*39*). More recently, Katada *et al*. have reported that gene expression levels of aldosterone synthase and cardiac aldosterone content are both elevated in MI hearts even in angiotensin II type 1A receptor–knockout mice (*40*). In various epithelial cells, expression of 11β-HSD2 converts endogenous glucocorticoids to their receptor-inactive 11-keto analogs, thereby conferring aldosterone selectivity on MR (*41*). Although cardiac myocytes express MR with high affinities for aldosterone, corticosterone and cortisol (*42*, *43*), cardiac expression of 11β-HSD2 is reported to be extremely low, indicating that myocyte MR are primarily occupied by endogenous glucocorticoids (*41*). Moreover, previous reports suggest the possibility that glucocorticoids do not activate MR but act as antagonists in nonepithelial cells such as myocytes (*44*, *45*). On the other hand, it was recently reported that overexpressing 11β-HSD2 in cardiac myocytes drives cardiac hypertrophy, fibrosis and heart failure, which phenotype is ameliorated by eplerenone, providing strong evidence that aldosterone signaling is directly involved in cardiac pathophysiology (*46*).

In the present study, besides an increase in collagen type I gene expression, both cardiac MR and 11β-HSD2 mRNA expression levels were upregulated by ≈2-fold even at 14 days after MI, and spironolactone significantly suppressed the expression of both genes. Several previous reports have demonstrated that expression of MR mRNA was significantly increased under pathological conditions, such as post-MI and heart failure (*47*, *48*). Indeed, *in vitro* studies have shown that aldosterone and α-adrenergic stimulation each significantly increases the expression of MR mRNA (*49*, *50*). Since the production of aldosterone and sympathetic nerve activity in cardiac tissues are enhanced under pathological conditions particularly after MI, it is reasonable to consider that these factors raise the expression of MR in cardiac tissue. In addition, previous data have shown that expression of 11β-HSD2 is negatively regulated by either nitric oxide or tumor necrosis factor (TNF)-α (*51*, *52*) but also is positively regulated by aldosterone (*53*). We have also confirmed that aldosterone significantly increases the expression of 11β-HSD2 in cultured rat neonatal cardiac myocytes (unpublished observation). Although there is not enough information to know which other factors might regulate expression levels of MR and 11β-HSD2 mRNA particularly in pathological hearts, we speculate that MI raises the expression of these genes through the production of aldosterone in cardiac tissue, and furthermore that spironolactone does not directly suppress expression of those genes but indirectly affects the expression of MR and 11β-HSD2 *via* the inhibitory action of MR in the infract hearts.

In conclusion, our data suggest several linked possible injurious pathways: 1) aldosterone can access cardiac MR in pathological conditions such as MI; 2) increased MR-mediated aldosterone signaling accelerates myocyte apoptosis and progresses expansion of the infarct area, ventricular dilatation and thinning of the ventricular wall, resulting in myocardial dysfunction; 3) spironolactone can inhibit aldosterone signaling mediated by MR, whose number and whose selectivity to

aldosterone were upregulated after MI. Our present data suggest the possibility that spironolactone prevents myocyte apoptosis and ventricular remodeling in post-infarct hearts. However, the remodeling process after MI involves a number of hemodynamic and neurohormonal alterations, which may complexly influence myocyte apoptosis. Therefore, it still remains as a study limitation to demonstrate the direct anti-apoptotic effect of spironolactone on cardiac myocytes in *in vivo* remodeling hearts. This issue should be further investigated in the future.

References

1. Pfeffer MA: Left ventricular remodeling after acute myocardial infarction. *Annu Rev Med* 1995; **46**: 455–466.
2. Tatsumi T, Shiraishi J, Keira N, *et al*: Intracellular ATP is required for mitochondrial apoptotic pathways in isolated hypoxic rat cardiac myocytes. *Cardiovasc Res* 2003; **52**: 428–440.
3. Fliss H, Gattinger D: Apoptosis in ischemic and reperfused rat myocardium. *Circ Res* 1996; **79**: 949–956.
4. Kajstura J, Cheng W, Reiss K, *et al*: Apoptotic and necrotic myocyte cell deaths are independent contributing variables of infarct size in rats. *Lab Invest* 1996; **74**: 86–107.
5. Cheng W, Kajstura J, Nitahara JA, *et al*: Programmed myocyte cell death affects the viable myocardium after infarction in rats. *Exp Cell Res* 1996; **226**: 316–327.
6. Olivetti G, Quaini F, Sala R, *et al*: Acute myocardial infarction in humans is associated with the activation of programmed myocyte cell death in the surviving portion of the heart. *J Mol Cell Cardiol* 1996; **28**: 2005–2016.
7. Beltrami CA, Finato N, Rocco M, *et al*: Structural basis of end-stage failure in ischemic cardiomyopathy in humans. *Circulation* 1994; **89**: 151–163.
8. Olivetti G, Abbi R, Quaini F, *et al*: Apoptosis in the failing human heart. *N Eng J Med* 1997; **336**: 1131–1141.
9. Saraste A, Pulkki K, Kallajoki M, *et al*: Cardiomyocyte apoptosis and progression of heart failure to transplantation. *Eur J Clin Invest* 1999; **29**: 380–386.
10. Packer M: The neurohormonal hypothesis: a theory to explain the mechanism of disease progression in heart failure. *J Am Coll Cardiol* 1992; **20**: 248–254.
11. Sato A, Saruta T: Aldosterone-induced organ damage: plasma aldosterone level and inappropriate salt status. *Hypertens Res* 2004; **27**: 303–310.
12. Pitt B, Zannad F, Remme WJ, *et al*: The effect of spironolactone on morbidity and mortality in patients with severe heart failure. *N Engl J Med* 1999; **341**: 709–717.
13. Pitt B, Remme W, Zannad F, *et al*, Eplerenone Post-Acute Myocardial Infarction Heart Failure Efficacy and Survival Study Investigators: Eplerenone, a selective aldosterone blocker, in patients with left ventricular dysfunction after myocardial infarction. *N Engl J Med* 2003; **348**: 1309–1321.
14. Mizuno Y, Yoshimura M, Yasue H, *et al*: Aldosterone production is activated in the failing ventricles in human. *Circulation* 2001; **103**: 72–77.
15. Yamamoto N, Yasue H, Mizuno Y, *et al*: Aldosterone is produced from ventricles in patients with essential hypertension. *Hypertension* 2002; **39**: 958–962.
16. Silvestre JS, Robert V, Heymes C, *et al*: Myocardial production of aldosterone and corticosterone in the rat: physiological regulation. *J Biol Chem* 1998; **273**: 4883–4891.
17. Struthers AD, MacDonald TM: Review of aldosterone- and angiotensin II–induced target organ damage and prevention. *Cardiovasc Res* 2004; **61**: 663–670.
18. Funder JW: Glucocorticoid and mineralocorticoid receptors: biology and clinical relevance. *Annu Rev Med* 1997; **48**: 231–240.
19. Slight SH, Ganjam VK, Gomez-Sanchez CE, Zhou MY, Weber KT: High affinity NAD^+-dependent 11β-hydroxysteroid dehydrogenase in the human heart. *J Mol Cell Cardiol* 1996; **28**: 781–787.
20. Mano A, Tatsumi T, Shiraishi J, *et al*: Aldosterone directly induces myocyte apoptosis through calcineurin-dependent pathways. *Circulation* 2004; **110**: 317–323.
21. Kobara M, Tatsumi T, Kambayashi D, *et al*: Effect of ACE inhibition on myocardial apoptosis in an ischemia-reperfusion rat heart model. *J Cardiovasc Pharmacol* 2003; **41**: 880–889.
22. Veliotes DGA, Woodiwiss AJ, Deftereos DAJ, Gray D, Osadchii O, Norton GR: Aldosterone receptor blockade prevents the transition to cardiac pump dysfunction induced by β-adrenoreceptor activation. *Hypertension* 2005; **45**: 914–920.
23. Bäcklund T, Palojoki E, Saraste A, *et al*: Effect of vasopeptide inhibitor omapatrilat on cardiomyocyte apoptosis and ventricular remodeling in rat myocardial infarction. *Cardiovasc Res* 2003; **57**: 727–737.
24. Delyani JA, Robinson EL, Rudolph AE: Effect of a selective aldosterone receptor antagonist in myocardial infarction. *Am J Physiol* 2001; **50**: H647–H654.
25. Brilla CG, Pick R, Tan LB, Janicki JS, Weber KT: Remodeling of the rat right and left ventricles in experimental hypertension. *Circ Res* 1990; **67**: 1355–1364.
26. Roussoulieres AL, Raisky O, Chalabreysse L, *et al*: Identification and characterization of two genes (MIP-1β, VE-CADHERIN) implicated in acute rejection in human heart transplantation: use of murine models in tandem with cDNA arrays. *Circulation* 2005; **111**: 2636–2644.
27. Delcayre C, Swynghedauw B: Molecular mechanisms of myocardial remodeling. The role of aldosterone. *J Mol Cell Cardiol* 2002; **34**: 1577–1584.
28. Solomon SD, Pfeffer MA: Aldosterone antagonism and myocardial infarction. From animals to man and back. *J Am Coll Cardiol* 2003; **42**: 1674–1676.
29. Zannad F, Alla F, Dousset B, Perez A, Pitt B, RALES Investigators: Limitation of excessive extracellular matrix turnover may contribute to survival benefit of spironolactone therapy in patients with congestive heart failure: insights from the Randomized Aldactone Evaluation Study (RALES). *Circulation* 2000; **102**: 2700–2706.
30. Suzuki G, Morita H, Mishima T, *et al*: Effects of long-term monotherapy with eplerenone, a novel aldosterone blocker, on progression of left ventricular dysfunction and remodeling in dogs with heart failure. *Circulation* 2002; **106**: 2967–2972.
31. Fraccarollo D, Galuppo P, Hildemann S, Christ M, Ertl G, Bauersachs J: Additive improvement of left ventricular

remodeling and neurohormonal activation by aldosterone receptor blockade with eplerenone and ACE inhibition in rats with myocardial infarction. *J Am Coll Cardiol* 2003; **42**: 1666–1673.
32. Hayakawa K, Takemura G, Kanoh M, *et al*: Inhibition of granulation tissue cell apoptosis during the subacute stage of myocardial infarction improves cardiac remodeling and dysfunction at the chronic stage. *Circulation* 2003; **108**: 104–109.
33. Wencker D, Chandra M, Nguyen K, *et al*: A mechanistic role for cardiac myocyte apoptosis in heart failure. *J Clin Invest* 2003; **111**: 1497–1504.
34. Foo RSY, Mani K, Kitsis RN: Death begets failure in the heart. *J Clin Invest* 2005; **115**: 565–571.
35. Cesselli D, Jakoniuk I, Barlucchi L, *et al*: Oxidative stress–mediated cardiac cell death is a major determinant of ventricular dysfunction and failure in dog dilated cardiomyopathy. *Circ Res* 2001; **89**: 279–286.
36. Chandrashekhar Y, Sen S, Anway R, Shuros A, Anand I: Long-term caspase inhibition ameliorates apoptosis, reduces myocardial troponin-I cleavage, protects left ventricular function, and attenuates remodeling in rats with myocardial infarction. *J Am Coll Cardiol* 2004; **43**: 295–301.
37. Leri A, Claudio PP, Li Q, *et al*: Stretch-mediated release of angiotensin II induces myocyte apoptosis by activating p53 that enhances the local renin-angiotensin system and decreases the Bcl-2-to-Bax protein ratio in the cell. *J Clin Invest* 1998; **101**: 1326–1342.
38. de Gasparo M, Joss U, Ramjoue HP, *et al*: Three new epoxy-spironolactone derivatives: characterization *in vivo* and *in vitro*. *J Pharmacol Exp Ther* 1987; **240**: 650–656.
39. Silvestre JS, Heymes C, Oubenaissa A, *et al*: Activation of cardiac aldosterone production in rat myocardial infarction. Effect of angiotensin II receptor blockade and role in cardiac fibrosis. *Circulation* 1999; **99**: 2694–2701.
40. Katada J, Meguro T, Saito H, *et al*: Persistent cardiac aldosterone synthesis in angiotensin II type 1A receptor–knockout mice after myocardial infarction. *Circulation* 2005; **111**: 2157–2164.
41. Funder JW, Pearce PT, Smith R, Smith AI: Mineralocorticoid action: target tissue specificity is enzyme, not receptor, mediated. *Science* 1988; **242**: 986–989.
42. Sheppard KE, Autelitano DJ: 11β-Hydroxysteroid dehydrogenase 1 transforms 11-dehydrocorticosterone into transcriptionally active glucocorticoid in neonatal rat heart. *Endocrinology* 2002; **143**: 198–204.
43. Lombes M, Oblin ME, Gasc JM, Baulieu EE, Farman N, Bonvalet JP: Immunohistochemical and biochemical evidence for a cardiovascular mineralocorticoid receptor. *Circ Res* 1992; **71**: 503–510.
44. Young M, Fullerton M, Dilley R, Funder J: Mineralocorticoids, hypertension, and cardiac fibrosis. *J Clin Invest* 1994; **93**: 2578–2583.
45. Sato A, Funder JW: High glucose stimulates aldosterone-induced hypertrophy *via* type 1 meneralocorticoid receptors in neonatal rat cardiomyocytes. *Endocrinology* 1996; **137**: 4145–4153.
46. Qin W, Rudolph AE, Bond BR, *et al*: Transgenic model of aldosterone-driven cardiac hypertrophy and heart failure. *Circ Res* 2003; **93**: 69–76.
47. Nagata K, Obata K, Xu J, *et al*: Mineralocorticoid receptor antagonism attenuates cardiac hypertrophy and failure in low-aldosterone hypertensive rats. *Hypertension* 2006; **47**: 656–664.
48. Konishi A, Tazawa C, Miki Y, *et al*: The possible roles of mineralocorticoid receptor and 11β-hydroxysteroid dehydrogenase type 2 in cardiac fibrosis in the spontaneously hypertensive rat. *J Steroid Biochem Mol Biol* 2003; **85**: 439–442.
49. Castren M, Trapp T, Berninger B, Castren E, Holsboer F: Transcriptional induction of rat mineralocorticoid receptor gene in neurones by corticosteroids. *J Mol Endocrinol* 1995; **14**: 285–293.
50. Lister K, Autelitano DJ, Jenkins A, Hannan RD, Sheppard KE: Cross talk between corticosteroids and alpha-adrenergic signalling augments cardiomyocyte hypertrophy: a possible role for SGK1. *Cardiovasc Res* 2006; **70**: 555–565.
51. Sun K, Yang K, Challis JR: Differential regulation of 11β-hydroxysteroid dehydrogenase type 1 and 2 by nitric oxide in cultured human placental trophoblast and chorionic cell preparation. *Endocrinology* 1997; **138**: 4912–4920.
52. Suzuki S, Tsubochi H, Ishibashi H, *et al*: Inflammatory mediators down-regulate 11β-hydroxysteroid dehydrogenase type 2 in a human lung epithelial cell line BEAS-2B and the rat lung. *Tohoku J Exp Med* 2005; **207**: 293–301.
53. Fukushima K, Funayama Y, Yonezawa H, *et al*: Aldosterone enhances 11β-hydroxysteroid dehydrogenase type 2 expression in colonic epithelial cells *in vivo*. *Scand J Gastroenterol* 2005; **40**: 850–857.